

# New austrolimulid from Russia supports role of Early Triassic horseshoe crabs as opportunistic taxa

Russell D.C. Bicknell<sup>1</sup> and Dmitry E. Shcherbakov<sup>2</sup>

<sup>1</sup> Palaeoscience Research Centre, School of Environmental and Rural Science, University of New England, Armidale, NSW, Australia

<sup>2</sup> Borissiak Paleontological Institute, Russian Academy of Sciences, Moscow, Russia

## ABSTRACT

Horseshoe crabs are extant marine euhelicerates that have a fossil record extending well into the Palaeozoic. Extreme xiphosurid morphologies arose during this evolutionary history. These forms often reflected the occupation of freshwater or marginal conditions. This is particularly the case for Austrolimulidae—a xiphosurid family that has recently been subject to thorough taxonomic examination. Expanding the austrolimulid record, we present new material from the Olenekian-aged Petropavlovka Formation in European Russia and assign this material to *Attenborolimulus superspinosus* gen. et sp. nov. A geometric morphometric analysis of 23 horseshoe crab genera illustrates that the new taxon is distinct from limulid and paleolimulid morphologies, supporting the assignment within Austrolimulidae. In considering Triassic austrolimulids, we suggest that the hypertrophy or reduction in exoskeletal sections illustrate how species within the family evolved as opportunistic taxa after the end-Permian extinction.

**Subjects** Evolutionary Studies, Paleontology, Taxonomy, Zoology

**Keywords** Xiphosurida, End-Permian extinction, Triassic recovery, Geometric morphometrics, New species, Exceptional preservation

Submitted 13 April 2021

Accepted 9 June 2021

Published 30 June 2021

Corresponding author

Russell D.C. Bicknell,  
rdcbicknell@gmail.com

Academic editor

Bruce Lieberman

Additional Information and  
Declarations can be found on  
page 16

DOI 10.7717/peerj.11709

© Copyright  
2021 Bicknell and Shcherbakov

Distributed under  
Creative Commons CC-BY 4.0

OPEN ACCESS

## INTRODUCTION

Examining ecological recovery from the “mother of all extinctions” (the end-Permian extinction) during the Triassic is important for understanding how biological systems can redevelop after major devastating events ([Erwin, Bowring & Yungan, 2002](#); [Jablonski, 2002](#); [Payne et al., 2004](#); [Twitchett et al., 2004](#); [Dineen, Fraiser & Sheehan, 2014](#)). Triassic vertebrate ([Hu et al., 2011](#); [Chen & Benton, 2012](#); [Benton et al., 2013](#); [Tintori et al., 2014](#); [Fu et al., 2016](#)), invertebrate ([Rodland & Bottjer, 2001](#); [Hu et al., 2011](#); [Chen & Benton, 2012](#); [Hofmann et al., 2013](#); [Fu et al., 2016](#); [Ponomarenko, 2016](#)), and trace ([Chen, Fraiser & Bolton, 2012](#); [Crasquin & Forel, 2014](#); [Luo & Chen, 2014](#); [Luo et al., 2019, 2020](#); [Shi et al., 2019](#); [Xing et al., 2021](#)) fossil assemblages have been examined to understand recovery of the distinct palaeoecological facets. The arthropod record in particular has shed light on how marine and terrestrial groups recovered after the end-Permian. Ostracods ([Crasquin-Soleau et al., 2007](#); [Forel, 2012](#); [Forel et al., 2013](#); [Crasquin & Forel, 2014](#); [Chu et al., 2015](#)) and insects ([Gall & Grauvogel-Stamm, 2005](#); [Shcherbakov, 2008a, 2008b](#); [Hu et al., 2011](#); [Żyła et al., 2013](#); [Ponomarenko, 2016](#); [Zheng et al., 2018](#)) are commonly

examined, with rarer studies of brachiopods ([Żyla et al., 2013](#)) and horseshoe crabs ([Gall & Grauvogel-Stamm, 2005](#); [Hu et al., 2011](#); [Lerner, Lucas & Lockley, 2017](#); [Bicknell et al., 2019b](#); [Bicknell, Hecker & Heyng, 2021](#)). The record of Triassic xiphosurids (so-called horseshoe crabs) has recently been scrutinised, a research trajectory that has uncovered a wealth of data on post-Permian taxa (see [Błażejowski et al., 2017](#); [Hu et al., 2017](#); [Lerner, Lucas & Lockley, 2017](#); [Bicknell et al., 2019a, 2019b, 2021](#); [Bicknell & Pates, 2020](#); [Lamsdell, 2020](#)). Two xiphosurid families are known from the Triassic: Austrolimulidae and Limulidae ([Table 1](#)). Of these two, austrolimulids are predominantly marginal marine to freshwater forms that commonly exhibit hypertrophied or reduced features. Here, we present new horseshoe crab material from the *Konservat Lagerstätte* within the Petropavlovka Formation, Cis-Urals of Russia to promote the study of Austrolimulidae and their role in the Triassic recovery of Xiphosurida. This material is also examined using geometric morphometrics to mathematically illustrate the austrolimulid position of these fossils within xiphosurid morphospace. This evidence, coupled with a thorough taxonomic consideration, prompted us to place the Petropavlovka Formation material within a novel genus and species: *Attenborolimulus superspinosus* gen. et sp. nov.

## Geological history and setting

The Permian–Triassic succession of the Cis-Urals is well known for diverse fossil tetrapods and stratigraphic sections that permit detailed study of changes in climate, landscapes, vegetation, and biological communities across the Permian–Triassic boundary ([Ochev & Shishkin, 1989](#); [Shishkin et al., 1995](#); [Benton, Tverdokhlebov & Surkov, 2004](#); [Gomankov, 2005](#); [Shcherbakov, 2008a](#); [Benton & Newell, 2014](#); [Shishkin & Novikov, 2017](#)). The Petropavlovka Formation within this important succession is considered upper Olenekian (251.2–247.2 Ma) based on the *Parotosuchus* Otshev & Shishkin (in [Kalandadze et al., 1968](#)) tetrapod fauna, the lungfish *Ceratodus multicristatus* ([Vorobyeva & Minikh, 1968](#)), miospore assemblages rich in *Densoisporites neburgii* associated with the lycophyte *Pleuromeia*, and magnetostratigraphy ([Fig. 1A](#); [Shishkin et al., 1995](#); [Minikh & Minikh, 1997](#); [Tverdokhlebov et al., 2003](#)). During the Olenekian, orogenic development occurred in the Ural Mountains, while the Peri-Caspian Depression was inundated by the transgression of the Palaeotethys. This resulted in increased rates of siliciclastic deposition in the Cis-Urals ([Tverdokhlebov, 1987](#)). In the Cis-Ural Trough and southeastern slope of the Volga-Ural Antecline, a vast lacustrine-deltaic floodplain was formed. This bordered the northern Peri-Caspian marine basin of the Palaeotethys. The Petropavlovka Formation accumulated in this floodplain. The formation consists of grey and reddish-grey siliciclastics. It is primarily a rhythmic alternation of coarse- and fine-grained sandstone, clay, siltstone, and fine-grained clayey sandstone, reaching a total thickness of 400–800 m ([Shishkin et al., 1995](#)). Conglomerate lenses are also common. Coarser sediment represents alluvial deposits, while finer lithologies constitute shallow water lacustrine deposits. These facies characterise the delta floodplain and delta front complexes that comprise the Petropavlovka Formation ([Tverdokhlebov et al., 2003](#)).

The Petropavlovka Formation stratotype section occurs along the Sakmara River and adjacent ravines close to Petropavlovka ~45 km north-east of Orenburg (52°02' N, 55°38' E).

**Table 1** Summary of known Triassic xiphosurids.

Taxon	Family	Formation, locality	Age	Depositional environment
<i>Austrolimulus fletcheri</i> Riek, 1955	Austrolimulidae	Hawkesbury Sandstone, New South Wales, Australia	Middle Triassic (Anisian, 247.2–242 Ma)	Marginal marine to freshwater
<i>Attenborolimulus superspinosus</i> gen. et sp. nov.	Austrolimulidae	Petropavlovka Formation, Cis-Urals, Russia	Early Triassic (Olenekian, 251.2–247.2 Ma)	Marginal marine to freshwater
<i>Batracholimulus fuchsbergensis</i> (Hauschke & Wilde, 1987)	Austrolimulidae	Exter Formation, Germany	Late Triassic (Rhaetian, 208.5–201.3 Ma)	Marginal marine to freshwater
<i>Dubbolimulus peetae</i> Pickett, 1984	Austrolimulidae	Ballimore Formation, New South Wales, Australia	Middle Triassic (Ladinian)	Marginal marine to freshwater
<i>Limulitella bronni</i> (Schimper, 1853)	?Austrolimulidae	Grés à Voltzia Formation, France	Middle Triassic (Anisian)	Marginal marine to freshwater
<i>Limulitella liasokeuperinus</i> (Braun, 1860)	?Austrolimulidae	?Exter Formation–?Bayreuth Formation, Germany	Late Triassic-Early Jurassic (?Rhaetian- Hettangian, 208.6–199.3 Ma)	Marginal marine to freshwater
<i>Limulitella tejraensis</i> Błażejowski et al., 2017	?Austrolimulidae	Ouled Chebbi Formation, Tunisia	Middle Triassic (Anisian-Early Ladinian, 247.2–237 Ma)	Marginal marine to freshwater
<i>Limulitella volgensis</i> Ponomarenko, 1985	?Austrolimulidae	Rybinsk Formation, Russia	Early Triassic (Olenekian)	Marine
<i>Psammolimulus gottingensis</i> Lange, 1923	Austrolimulidae	Solling Formation, Germany	Early Triassic (Olenekian, Spathian, 251.2–247.2 Ma)	Marginal marine to freshwater
<i>Vaderlimulus tricki</i> Lerner, Lucas & Lockley, 2017	Austrolimulidae	Thaynes Group, Idaho, USA	Early Triassic (Olenekian, Spathian)	Marginal marine
<i>Heterolimulus gadeai</i> (Vía & De Villalta, 1966)	Limulidae	Alcover Limestone Formation, Spain	Middle Triassic (Ladinian)	Marine
<i>Keuperlimulus vicensis</i> (Bleicher, 1897)	Limulidae	Marnes Irisées Supérieures Formation, France	Late Triassic	Marine
<i>Mesolimulus cespelli</i> Vía Boada, 1987	Limulidae	Alcover Limestone Formation, Spain	Middle Triassic (Ladinian)	Marine
<i>Sloveniolimulus rukini</i> Bicknell et al., 2019b	Limulidae	Strelovec Formation, Slovenia	Middle Triassic (Anisian)	Marine
<i>Tarracolimulus rieki</i> Romero & Vía Boada, 1977	Limulidae	Alcover Limestone Formation, Spain	Middle Triassic (Ladinian)	Marine
<i>Yunnanolimulus (?) henkeli</i> (von Fritsch, 1906)	Limulidae	Jena Formation, Germany	Middle Triassic (Anisian)	Marine
<i>Yunnanolimulus luopingensis</i> Zhang et al., 2009	Limulidae	Guanling Formation, Luoping, China	Middle Triassic (Anisian)	Marine

**Note:**

Taxa are ordered by family and then alphabetically by genus and species. Temporal data taken from Bicknell & Pates (2020), Bicknell, Naugolnykh & Brougham (2020), Bicknell et al. (2021) and Bicknell, Hecker & Heyng (2021). Note the uncertain placement of *Limulitella* in Austrolimulidae, and *Yunnanolimulus henkeli*. In Fig. 10 and Supplemental Information 3, *Limulitella* is placed within Limulidae, and *Yunnanolimulus (?) henkeli* is referred to *Limulitella henkeli* (following Bicknell et al., 2021).

Red beds exposed here yield tetrapods, lungfish, clam shrimps (conchostracans), and ostracods (Shishkin et al., 1995). Along one ravine, a one-meter-thick lens of grey fine-grained polymictic siltstone to sandstone was identified (locality Petropavlovka III, bed 43; Tverdokhlebov, 1967). The lens contains abundant plant megafossils including sphenophytes and gymnosperms (Dobruskina, 1994). In 2018–2019 numerous diverse

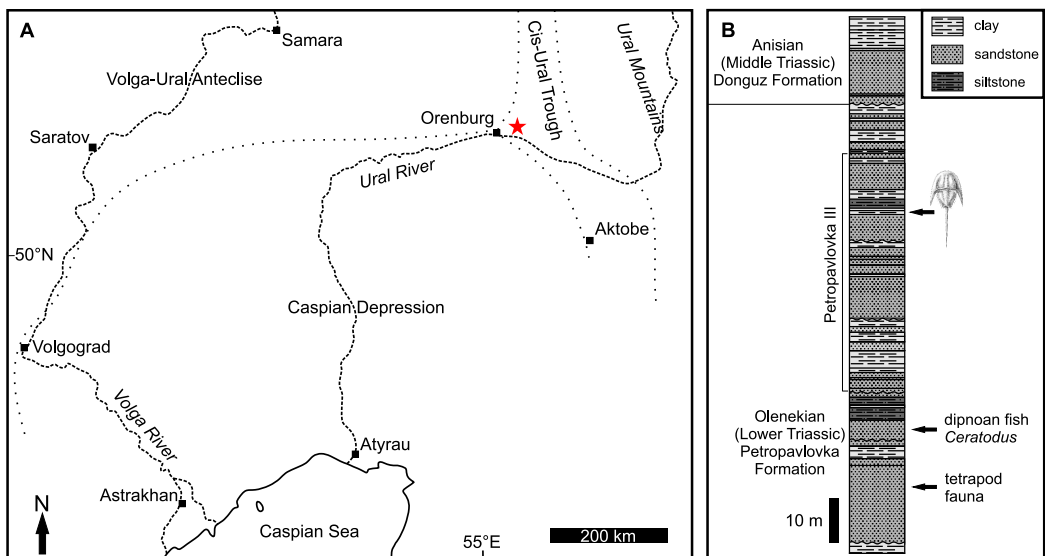


**Figure 1** Geographical and geological information for the studied fossil site. (A) Map showing locality of Petropavlovka III (red star). Dotted line represents boundaries of tectonic regions, modified from *Shcherbakov, Vinn & Zhuravlev (2021)*. (B) Stratigraphic log of Petropavlovka II–IV sections showing location of horseshoe crab-bearing lens (modified from *Tverdokhlebov, 1967*).

Full-size DOI: 10.7717/peerj.11709/fig-1

insects wings, millipedes, horseshoe crabs, microconchids, and a microdrile oligochaete were collected in the lens, along with seed fern pinnules and lycophyte fragments (*Hannibal & Shcherbakov, 2019*; *Shcherbakov et al., 2020*; *Shcherbakov, Vinn & Zhuravlev, 2021*).

## MATERIALS AND METHODS

The studied specimens were collected by the field parties of, and are housed in, the Borissiak Paleontological Institute (PIN), Russian Academy of Sciences, Moscow, Russia. The material was photographed with a Nikon D800 camera mounted with a Nikon AF-S ED Micro Nikkor 60 mm f/2.8G lens. Images were z-stacked with Helicon Focus Pro 6.7. Furthermore, a Leica DFC425 camera coupled to Leica M165C stereomicroscope was used. Finally, to examine possible evidence for finer structures, specimens were examined under a TESCAN VEGA scanning electron microscope (SEM) housed at the PIN. A backscattered electron detector was used as the specimens were not coated.

When describing the material, we followed the systematic taxonomy of *Bicknell & Pates (2020)* and *Bicknell et al. (2021)* and used anatomical terms presented in *Lerner, Lucas & Lockley (2017)*, *Bicknell (2019)*, *Bicknell, Naugolnykh & Brougham (2020)*, and *Bicknell et al. (2021)*.

The geometric morphometric analysis presented here develops on recent applications by *Bicknell (2019)*, *Bicknell & Pates (2019)*, *Bicknell et al. (2019b)*, and *Lustri, Laibl & Bicknell (2021)*. The approach was used to assess where the Petropavlovka Formation material falls in xiphosurid morphospace and allows for a mathematical comparison with other xiphosurid specimens, augmenting the taxonomic description presented here. A total of 103 specimens arrayed across 23 genera from Austrolimulidae, Limulidae,

and Paleolimulidae (sensu [Bicknell & Pates, 2020](#)) were considered. Landmarking and semilandmarking was conducted with the Thin-Plate Spline (TPS) suite (<http://life.bio.sunysb.edu/morph/index.html>). A TPS file was constructed using tpsUtil64 (v.1.7). The TPS file was imported into tpsDig2 (v.2.26). This software was used to place four landmarks on the right prosomal section, as well as 50 semi-landmarks along the right prosomal shield border ([Fig. 2](#); [Table S1](#)). Points were digitised as *xy* coordinates. When the right side was poorly preserved, the left side was used, and data mirrored. These points populated the TPS file with landmark data ([Supplemental Information 1](#)). The TPS file was imported into R. The ‘geomorph’ package ([Adams, Collyer & Kaliontzopoulou, 2020](#)) was used to conduct a Procrustes Superimposition and Principal Components Analysis (PCA) of the data ([Supplemental Information 2](#)). Only the first two Principal Components (PCs) were considered as they explain 75.6% of the variation in the data ([Supplemental Information 3](#)). [Bicknell et al. \(2019b\)](#) demonstrated that the distribution in PC space reflects biological variation. As such, while preservational mode varies between specimens (consider [Bicknell & Pates, 2020](#)), this variation has little impact on the morphospace (see discussion in [Lustri, Laibl & Bicknell, 2021](#)). The generic and family assignments presented in [Supplemental Information 3](#) reflect a combination of taxonomic theses presented in [Bicknell & Pates \(2020\)](#), [Lamsdell \(2020\)](#), and [Bicknell et al. \(2021\)](#).

The electronic version of this article in Portable Document Format (PDF) will represent a published work according to the International Commission on Zoological Nomenclature (ICZN), and hence the new names contained in the electronic version are effectively published under that Code from the electronic edition alone. This published work and the nomenclatural acts it contains have been registered in ZooBank, the online registration system for the ICZN. The ZooBank LSIDs (Life Science Identifiers) can be resolved and the associated information viewed through any standard web browser by appending the LSID to the prefix <http://zoobank.org/>. The LSID for this publication is: 5435A6BA-AE34-4698-8872-7A350DB799B1. The online version of this work is archived and available from the following digital repositories: PeerJ, PubMed Central and CLOCKSS.

## Systematic Palaeontology

Family Austrolimulidae [Riek, 1955](#)

Genus *Attenborolimulus* gen. nov.

**Etymology:** The generic name is given in honour of Sir David Attenborough and his unparalleled contributions to natural history and conservation. His last name is combined with *Limulus*—the most-well documented extant xiphosurid genus.

**Type species:** *Attenborolimulus superspinosus*, new species.

**Diagnosis.** Austrolimulid with anteriorly effaced, ridge-less cardiac lobe, slightly splayed genal spines extending posteriorly to three-fourths of thoracetrone length with occipital bands extending to spine terminus, tubercle structures along posterior prosomal and anterior thoracetrone border, medial thoracetrone lobe lacking a sagittal ridge, and long, strongly keeled telson.

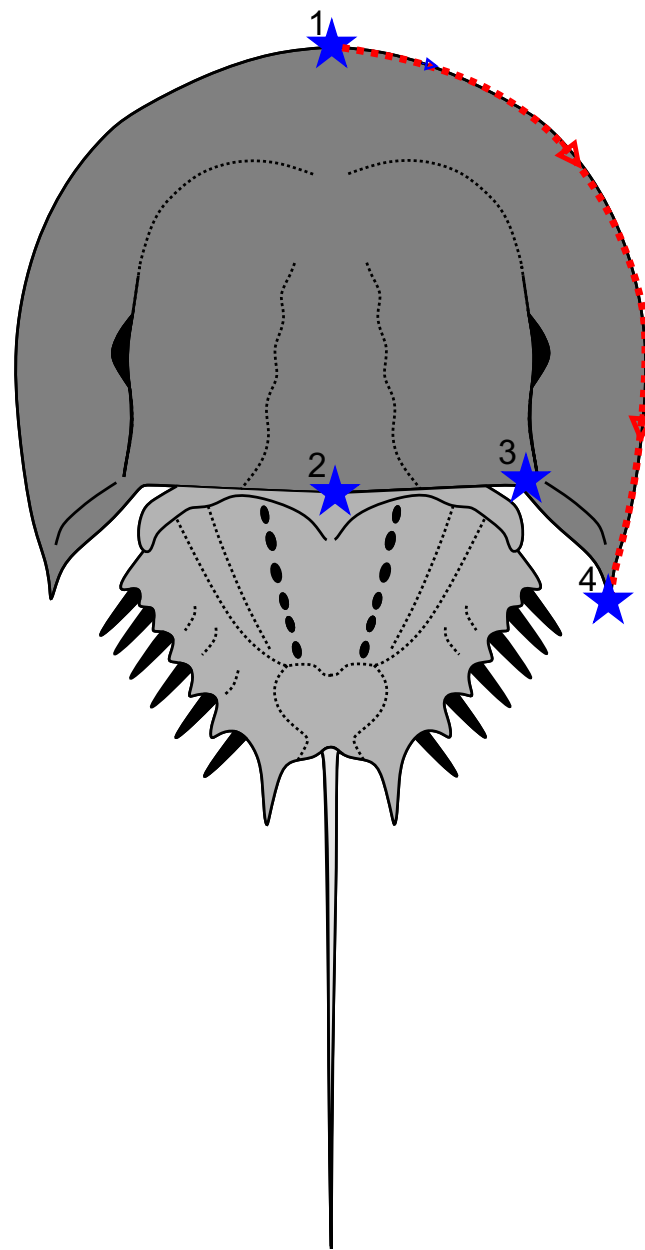


**Figure 2** Depiction of geometric morphometric data gathered here: four landmarks and one semilandmark outline. Consider Table S1 for description of landmarks.

[Full-size](#) DOI: 10.7717/peerj.11709/fig-2

*Attenborolimulus superspinosus* sp. nov.

[Figures 3–8](#)

**Etymology:** Species name reflects the hypertrophied (*super-*) genal spine (*-spinosis*) morphology.

**Holotype:** PIN 5640/220 (part and counterpart).

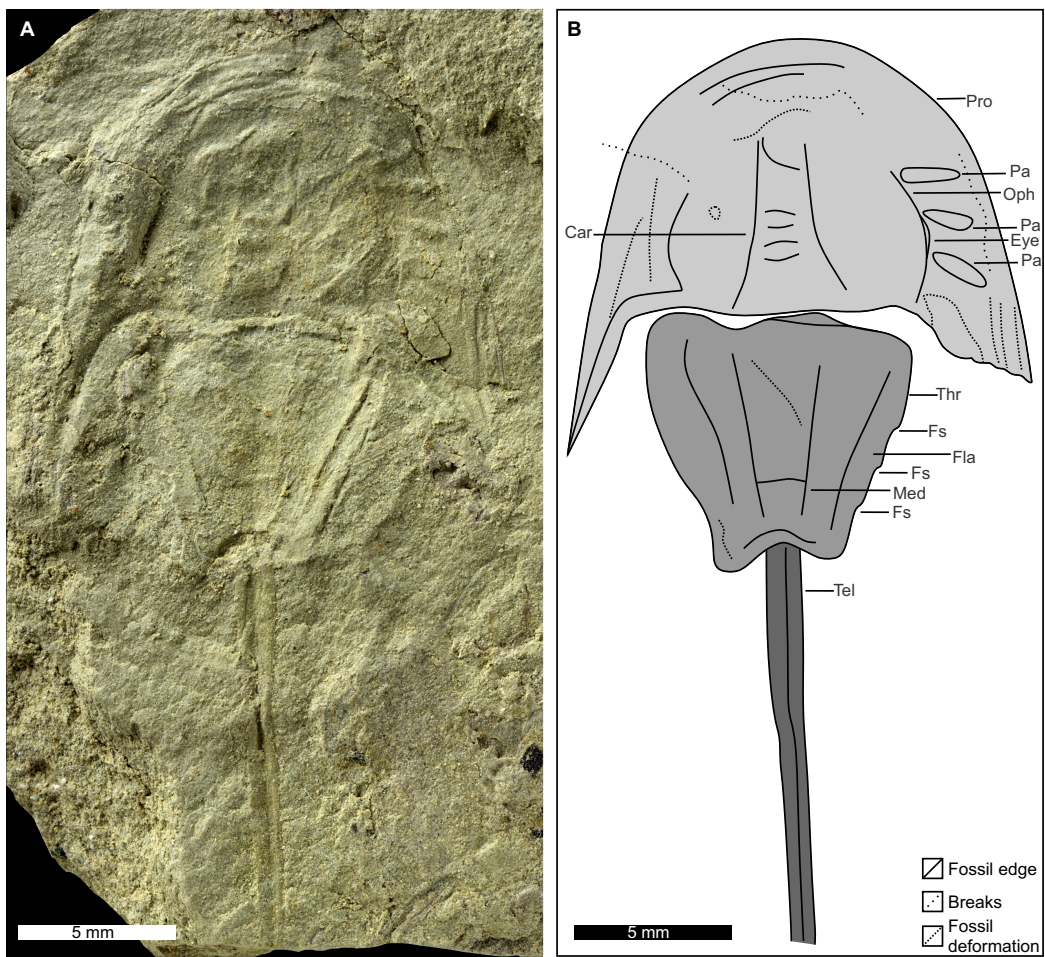


**Figure 3** Holotype of *Attenborolimulus superspinosus* gen. et sp. nov. PIN 5640/220, counterpart. (A and B): Photograph and interpretative drawing. Abbreviations: Car: cardiac lobe; Eye: lateral compound eye; Fla: thoracetronic flange; Fs: fixed spine; Med: medial thoracetronic lobe; Oph: ophthalmic ridge; Pa: prosomal appendage; Pro: prosoma; Thr: thoracetrone; Tel: telson. Image credit: Sergey Bagirov.

[Full-size](#) DOI: [10.7717/peerj.11709/fig-3](https://doi.org/10.7717/peerj.11709/fig-3)

**Paratypes:** PIN 5640/217, PIN 5640/200 (part and counterpart).

**Type locality and horizon.** Petropavlovka III near the village of Petropavlovka, Orenburg region, Russia; Petropavlovka Formation, upper Olenekian, Lower Triassic.

**Diagnosis.** Same as for genus.

**Preservation.** Specimens are preserved as partly domed exoskeletons as part and counterpart on yellowish or grey siltstone.

**Description.** PIN 5640/220 (part and counterpart): An articulated prosoma, thoracetrone, and distally incomplete telson (Figs. 3–5). Specimen is 32.0 mm long as preserved. Prosoma parabolic in outline, 9.8 mm long at midline, and 15.3 mm wide between genal spine tips. Exoskeletal warping along anterior and left lateral prosomal sections. Prosomal rim 0.2 mm wide. Prosomal doublure 1.6 mm wide laterally, arcuately widened

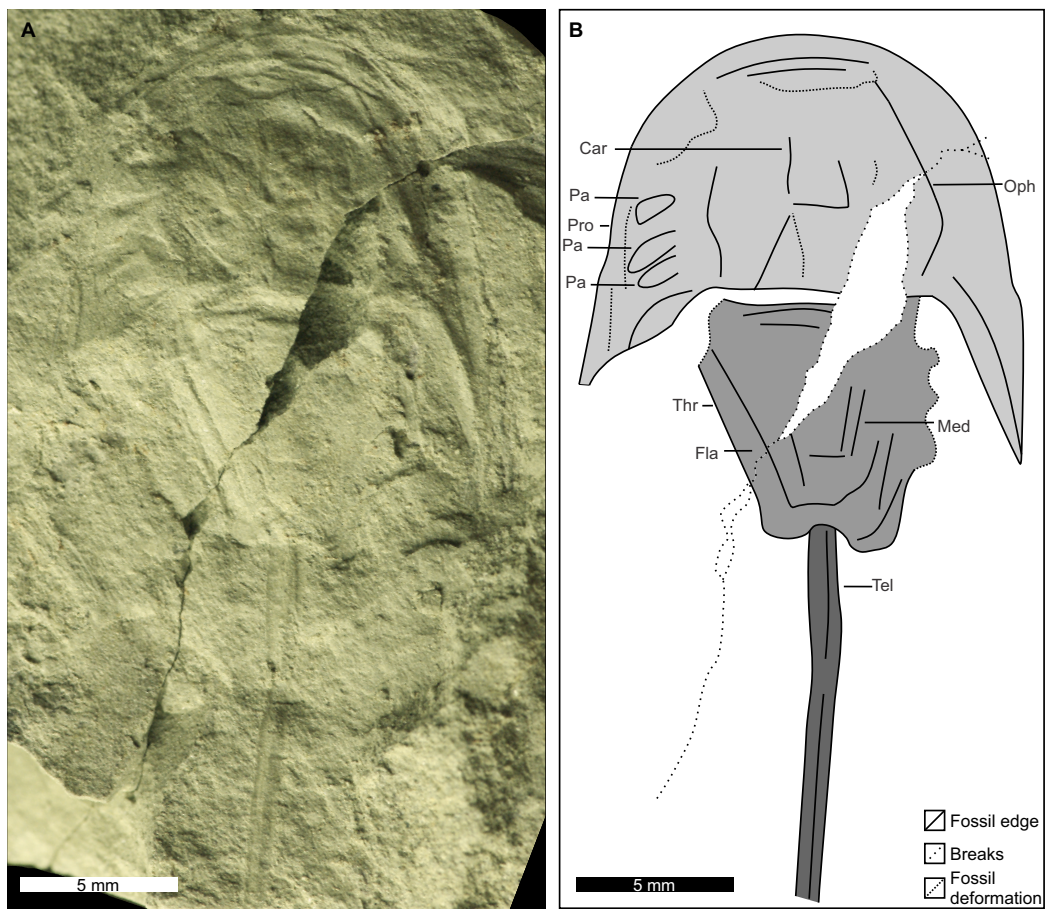


**Figure 4** Holotype of *Attenborolimulus superspinosus* gen. et sp. nov., PIN 5640/220, part. (A and B): Photograph and interpretative drawing. Abbreviations: Car: cardiac lobe; Fla: thoracetrone flange; Med: medial thoracetrone lobe; Oph: ophthalmic ridge; Pa: prosomal appendage; Pro: prosoma; Thr: thoracetrone; Tel: telson. Image credit: Dmitry Shcherbakov. [Full-size](#) DOI: 10.7717/peerj.11709/fig-4

to 2.5 mm medially. Ophthalmic ridges curved towards the lateral prosomal border, ~4.5 mm long. Ridges do not converge anteriorly. Lateral compound eyes narrow and reniform, ~2.9 mm long, ~0.7 mm wide, inner orbita 4.1 mm from midline. Cardiac lobe 7.5 mm long, 4.1 mm wide posteriorly, tapering to its mid-length, about 2.0 mm wide in anterior half, tapered to 1.4 mm near apex, effaced anteriorly. Break in left genal spine within first quarter of thoracetrone. Posterior-most left genal section 8.4 mm from midline. Angle between inner edge of left genal spine and left thoracetrone side 77.2°. Right genal spine complete, terminates three fourths along thoracetrone. Genal spine terminus 7.8 mm from midline, 6.9 mm from level of prosomal-thoracetrone hinge. Angle between right inner edge of genal spine and right thoracetrone side 38.5°. Pronounced occipital bands extend from ophthalmic ridges to genal spine ends. Prosomal-thoracetrone hinge pronounced, 7.6 mm wide, and 0.6 mm long. Posterior prosomal border with shallow central notch 2.1 mm wide. Distal sections of prosomal appendages noted lateral to compound eyes (Fig. 3B).

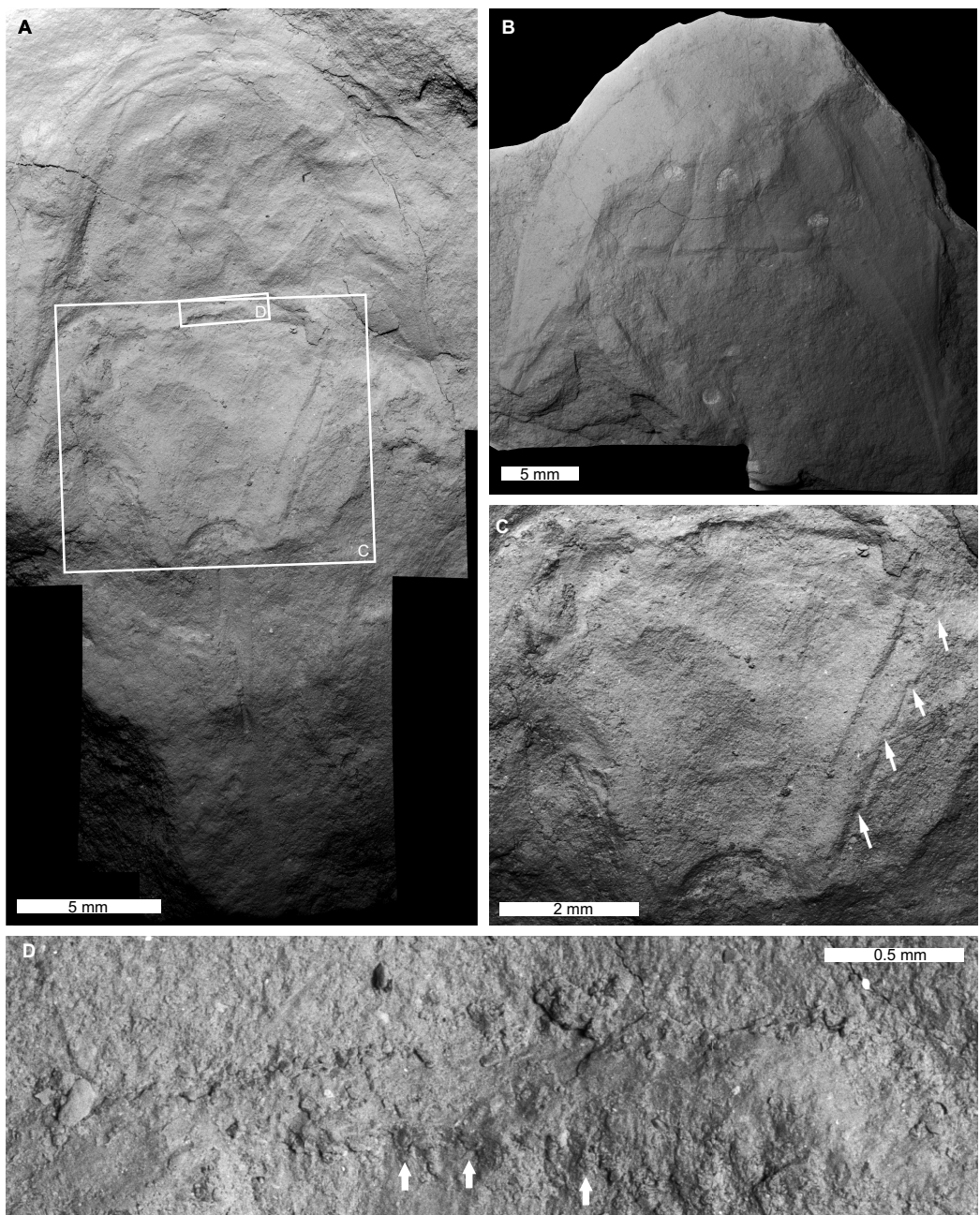


**Figure 5** SEM images of the *Attenborolimulus superspinosus* gen. et sp. nov. (A, C and D): Holotype, PIN 5640/220, counterpart. (A) Entire specimen. (C) Close up of box in (A), showing small moveable spine notches and fixed spines (white arrows). (D): Close up of box in (A), showing tubercles along prosomal thoracetrone border (white arrows). (B): Paratype, PIN 5640/200, part. Image credit: Dmitry Shcherbakov.

[Full-size](#) DOI: 10.7717/peerj.11709/fig-5

Thoracetrone trapezoidal, completely preserved in counterpart (Figs. 3 and 5C), 8.1 mm long at midline, 9.4 mm wide anteriorly, tapering to 4.7 mm posteriorly. Tubercl structures along anterior thoracetrone border noted under SEM (Fig. 5D). Thoracetrone flange present. Rounded anterolateral lobes apparently present. Setose margins of branchial appendages (opercula) visible anteriorly on left side in counterpart. Medial

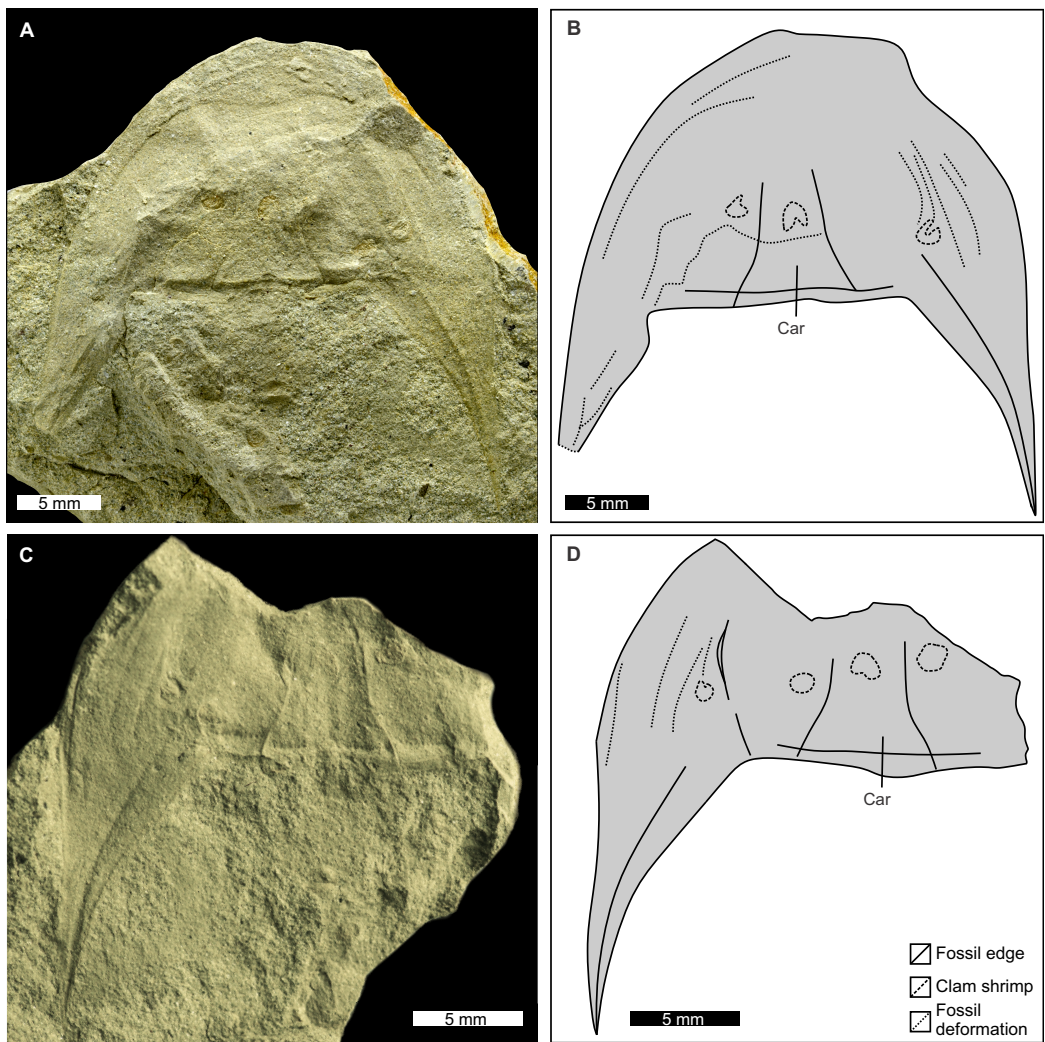


**Figure 6** Paratype PIN 5640/200 of *Attenborolimulus superspinosus* gen. et sp. nov. showing key prosomal features. (A and B): Part, photograph and interpretative drawing. (C and D): Counterpart, photograph and interpretative drawing. Abbreviation: Car: cardiac lobe. Image credit: (A) Sergey Bagirov; (C) Dmitry Shcherbakov.

[Full-size](#) DOI: 10.7717/peerj.11709/fig-6

thoracetronic lobe weakly defined, 7.3 mm long, 3.0 mm anteriorly, tapering to 1.2 mm posteriorly. Lobe lacking medial thoracetronic ridge. Left pleural lobe has 0.3 mm wide rim. Left lobe 8.0 mm long, 2.6 mm wide, tapering posteriorly to short, round terminal spine. Right lobe damaged in part. Measurements taken from counterpart. Right lobe 8.2 mm long, 2.5 mm wide, tapering posteriorly to short, rounded terminal spine. Minute fixed spines and movable spine notches observed under SEM on left side of thoracetron (Fig. 5C). Telson 14.1 mm long as preserved, with well-developed keel. Telson terminates at rock edge, has a kink at a third of the spine length.

PIN 5640/200 (part and counterpart): Isolated prosoma preserved more completely in part (Figs. 5B and 6). Prosoma parabolic in outline, 15.1 mm long at midline, and 28.0 mm wide between most distal genal spine points. Exoskeletal warping along anterior and right lateral prosomal sections. Prosomal rim 0.6 mm wide. Prosomal doublure 2.1 mm

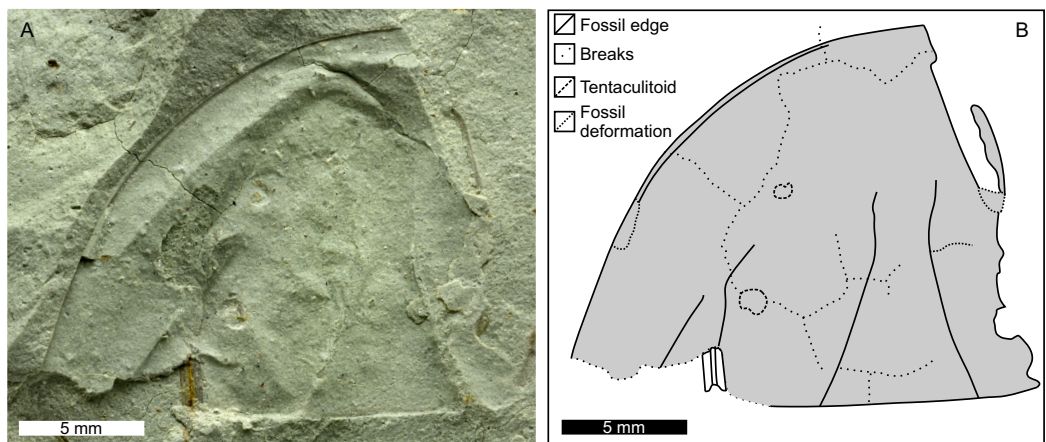


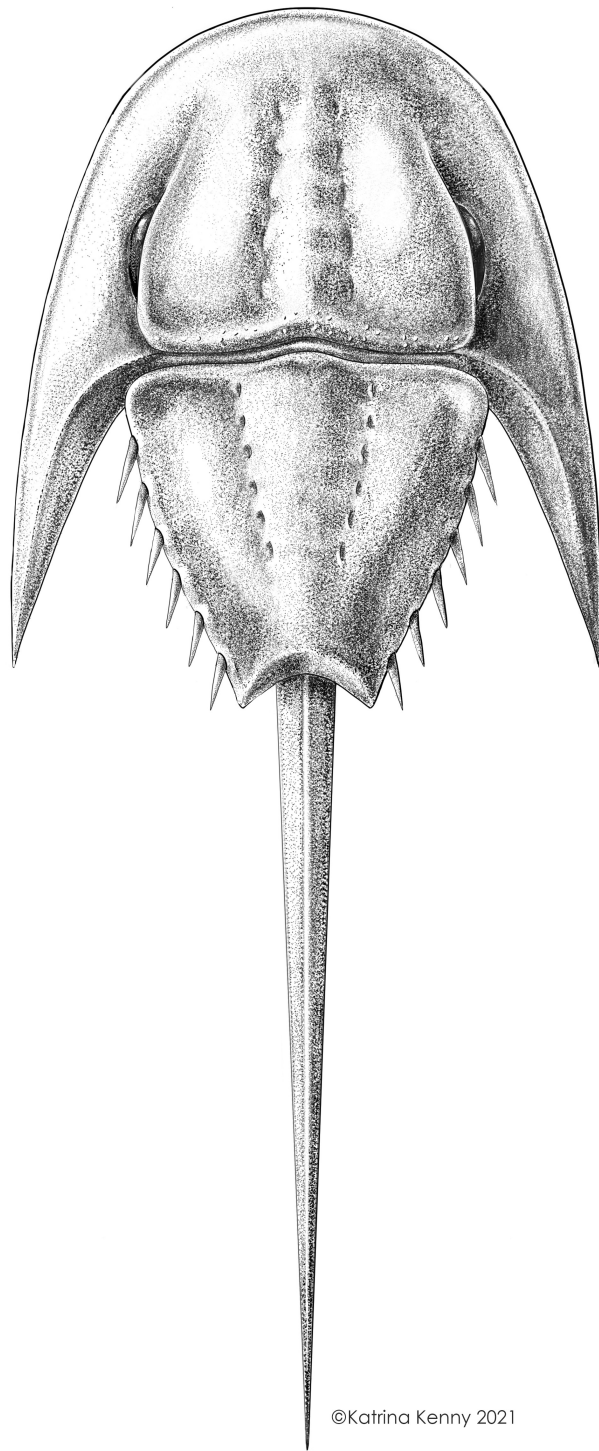
**Figure 7** Paratype PIN 5640/217 of *Attenborolimulus superspinosus* gen. et sp. nov. (A and B): Photograph and interpretative drawing. Image credit: Sergey Bagirov.

[Full-size](#) DOI: [10.7717/peerj.11709/fig-7](https://doi.org/10.7717/peerj.11709/fig-7)

wide, arcuately widened backwards up to 4.1 mm medially. Right ophthalmic ridge noted in counterpart (Figs. 6C and 6D). Ridge curved towards the lateral prosomal border, 9.1 mm long. Lateral compound eyes narrow reniform, ~3.7 mm long, ~0.8 mm wide, right inner orbita 7.5 mm from midline. Cardiac lobe present, 7.5 mm long, 6.8 mm wide posteriorly, tapering (posteriorly to anteriorly) to 1.8 mm, effaced anteriorly. Left genal spine broken distally. Most distal left genal section 13.9 mm from midline. Right genal spine complete, lateral margin slightly convex. Genal spine terminus 14.1 mm from midline, 13.6 mm from prosomal-thoracetrone hinge. Pronounced occipital bands extend from ophthalmic ridges to genal spine ends, better preserved along right genal spine. Ridge delimiting occipital band with tubercles along posterior prosomal border and near base of genal spines. Posterior prosomal border with arcuate central notch 4.3 mm wide. Clam shrimp (round structures) noted.

PIN 5640/217: Central and left side of prosoma (Fig. 7), 15.4 mm long at midline, and 17.1 mm wide at widest section. Prosomal rim 0.3 mm wide. Partial left ophthalmic ridge noted. Cardiac lobe 9.0 mm long, 7.0 mm wide posteriorly, tapering slightly anteriorly to 2.5 mm, effaced anteriorly. Anterior most section of left genal spine noted. Two tentaculitoid tubeworms noted on left side of prosoma (round structures; Shcherbakov, Vinn & Zhuravlev, 2021).

**Remarks:** The horseshoe crab material documented herein displays hypertrophied genal spines, a feature common in Belinurina and Austrolimulidae. The examined material lacks the expression of thoracetrone tergites extending from the medial lobe to the thoracetrone edge and a rounded thoracetrone common to Belinurina. This suggests the material likely belongs within Austrolimulidae. Bicknell, Naugolnykh & Brougham (2020) outlined two major groupings of austrolimulids: those with reduced thoracetrone sections relative to the prosoma and those with genal spines that extend up to the thoracetrone terminus. Prosomal and thoracetrone sections of the Petropavlovka Formation specimens



©Katrina Kenny 2021

**Figure 8** Reconstruction of *Attenborolimulus superspinosus* gen. et sp. nov. Reconstruction credited to Katrina Kenny.

[Full-size](#) DOI: 10.7717/peerj.11709/fig-8

are comparable, excluding this material from the first group *Bicknell, Naugolnykh & Brougham (2020)* outlined. This differentiates the material considered here from *Batracholimulus fuchsbergensis* (*Hauschke & Wilde, 1987*), *Boeotiaspis longispinus* (*Schram, 1979*), *Dubbolimulus peetae* (*Pickett, 1984*), *Panduralimulus babcocki* (*Allen & Feldmann, 2005*), and *Shpineviolimulus jakovlevi* (*Glushenko & Ivanov, 1961*). Comparisons to *Austrolimulus fletcheri* (*Riek, 1955*), *Franconiolimulus pochankei* (*Bicknell, Hecker & Heyng, 2021*), *Psammolimulus gottingensis* (*Lange, 1923*), *Tasmaniolimulus patersoni* (*Bicknell, 2019*), and *Vaderlimulus tricki* (*Lerner, Lucas & Lockley, 2017*) are therefore needed, as they are austrolimulids with hypertrophied genal spines. *Austrolimulus fletcheri* and *V. tricki* both have hypertrophied genal spines with extensive splay, which is not observed in the Petropavlovka Formation material (*Riek, 1955, 1968; Lerner, Lucas & Lockley, 2017*). *Franconiolimulus pochankei*, the youngest austrolimulid, has a cardiac ridge, distally effaced occipital bands, and a thoracetrone free lobe, none of which are observed in the Petropavlovka Formation material. *Tasmaniolimulus patersoni* has pronounced thoracetrone free lobes, as well as keeled cardiac and medial thoracetrone lobes (*Ewington, Clarke & Banks, 1989; Bicknell, 2019*). These are not observed in the Petropavlovka Formation material, excluding the new fossils from this Lopingian (259.1–251.9 Ma) genus. *Psammolimulus gottingensis* is the most morphologically similar to the new material. Indeed, the genal spine morphology and pronounced occipital bands suggest a strong alignment with *P. gottingensis* (*Meischner, 1962*). However, *P. gottingensis* has hypertrophied terminal thoracetrone spines and pronounced free lobes. Neither of these features are observed in the specimens examined here. Based on this comparison, we assert that the Petropavlovka Formation material is morphologically distinct from other austrolimulids enough to be separated at the generic level, as *Attenborolimulus superspinosus* gen. et sp. nov. This taxonomic assessment is supported by geometric morphometric results (see “Results”).

One point to consider is *Limulitella Størmer, 1952* as an austrolimulid genus. *Lamsdell (2020)* recently used tree topology to propose that *Limulitella* fell into Austrolimulidae, suggesting that the family consisted of limuloids with “apodemal pits present on thoracetrone; thoracetrone lacking tergopleural fixed spines; posteriormost thoracetrone tergopleurae swept back and elongated to form ‘swallowtail’; axis of thoracetrone bearing dorsal keel” (*Lamsdell, 2020*, p. 20). Examining *L. bronni* (*Schimpfer, 1853*), for example, specimens have evidence of fixed spines, rendering the placement of *Limulitella* within Austrolimulidae tenuous. This perspective is supported by the position of *Limulitella* within morphospace that has consistently been closer to members of Limulidae of Paleolimulidae than Austrolimulidae (*Bicknell, 2019; Bicknell et al., 2019b; Bicknell & Pates, 2019*; Figs. 9 and 10). It therefore seems more likely that *Limulitella* species represent a group of limulids, rather than austrolimulids (sensu *Bicknell & Pates, 2020; Bicknell et al., 2021*). At best, *Limulitella* may represent a transitional form between the two families. Finally, comparing the morphologies of *Limulitella* presented in *Bicknell & Pates (2020, figs. 28–30)* to our material, the lack of hypertrophied genal spines separates this genus from *Attenborolimulus superspinosus*.

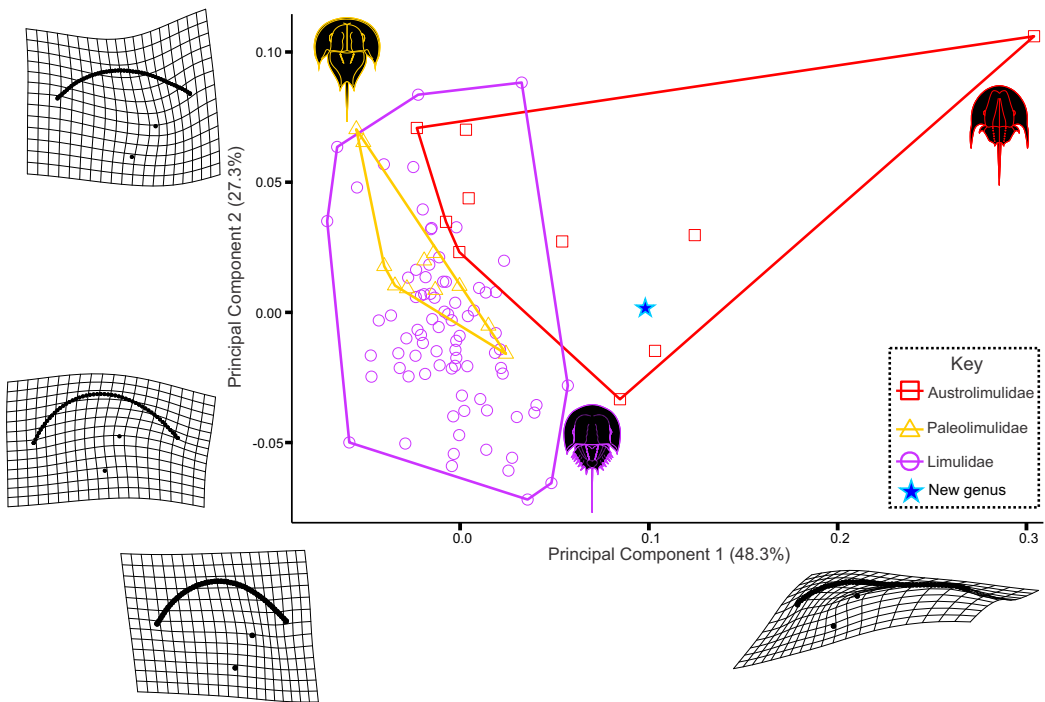


**Figure 9** Three examined xiphosurid families in PC space. Austrolimulids occupy most positive PC1 space while limulids and paleolimulids are mostly constrained to negative PC1 space. *Attenborolimulus superspinosus* gen. et sp. nov. falls within the convex hull occupied by Austrolimulidae. Note that the austrolimulid morphospace excludes *Limulitella* specimens, as the position of this genus in Austrolimulidae is considered dubious.

Full-size DOI: 10.7717/peerj.11709/fig-9

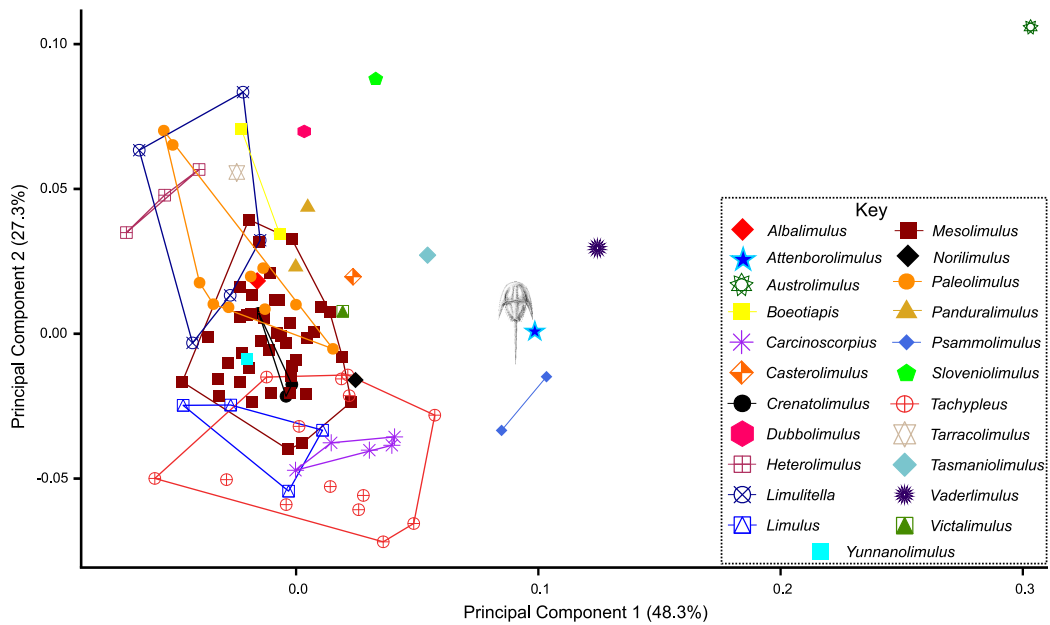


**Figure 10** PC plot showing morphospace occupied by xiphosurid genera. Where more than one specimen of the same genus was digitised, genera are bound by convex hulls. *Attenborolimulus superspinosus* gen. et sp. nov. is not bound by any convex hull, excluding the specimen from other genera.

Full-size DOI: 10.7717/peerj.11709/fig-10

## RESULTS

The PCA plot illustrates that PC1 (48.3% shape variation) describes how laterally the most distal genal spine point extends from the sagittal line (Fig. 9). PC2 (27.3% shape variation) describes how posteriorly the genal spine projects, relative to the prosomal sagittal line and posterior border. Paleolimulids and limulids are both located in PC1 space  $<0.05$ , reflecting the lack of genal splay observed in the groups. Specimens within Austrolimulidae cover PC1 space from 0–0.3 reflecting the variation in genal spine splay observed in the family. The holotype of *Attenborolimulus superspinosus* gen. et sp. nov. is located in a positive PC1 space ( $PC1 = 0.099$ ) and a neutral PC2 space ( $PC2 = 0.002$ ) (Figs. 9 and 10). It therefore falls outside the morphospace occupied by Limulidae and Paleolimulidae (Fig. 9) and within the morphospace occupied by Austrolimulidae. Furthermore, it is distinct from the distribution of other austrolimulid genera (Fig. 10).

## DISCUSSION

The meter-thick lens that yielded *Attenborolimulus* gen. nov. is a rare occurrence of grey lithologies among the red beds of the Petropavlovka Formation. The red beds yield the lungfish *Ceratodus*, temnospondyl amphibians, and procolophonid and erythrosuchid reptiles (Shishkin et al., 1995; Novikov, 2018). By comparison, the grey lens contain a different set of fossils: abundant, but fragmentary vascular plants, numerous insects (mainly isolated wings of various roaches, beetles, hemipterans, and rare dragonflies, grylloblattids, and orthopterans), microconchids, rare millipedes, and a microdrile oligochaete (Hannibal & Shcherbakov, 2019; Shcherbakov et al., 2020; Shcherbakov, Vinn & Zhuravlev, 2021). Clam shrimp and ostracods recorded in the grey bed occur in surrounding red beds as well. Notably, plant and animal fossils are not restricted to certain bedding planes but are randomly distributed in the rock, thus preserving some three-dimensionality. Such sediment probably accumulated in an ephemeral pond during a flood event. The millipedes, most plants, and nearly all insects were washed into the water body from the land and are therefore allochthonous fossils. The horsetails *Equisetites* and *Neocalamites* likely grew as helophytes protruding out of the water as some fragments of their stems are encrusted with microconchid shells. The aquatic ecosystem is represented by (sub)autochthonous fossils of ceratodontid lungfishes, numerous schizophoroid beetle adults, clam shrimp, ostracods, horseshoe crabs, microdriles, and microconchids. The microdrile specimens represent the earliest fossil record of oligochaete annelids. This small worm is similar to modern tubificids, and its relatively well-developed body wall musculature suggests that sediment burrowing was originally another way to escape desiccation on the bottom of seasonally drying ponds (Shcherbakov et al., 2020). Minute microconchids that encrusted plant stems, horseshoe crab exuvia, and other available firm substrates represent the major suspension feeders in the Petropavlovka ecosystem. These extinct lophophorates were genuine disaster taxa—eurytopic stress-tolerators that flourished in the aftermath of the end-Permian extinction in both marine and continental basins all over the world (Shcherbakov, Vinn & Zhuravlev, 2021). Dense accumulations of primarily pyrite dodecahedra are common on the plant stem fragments and attached microconchid tubes. A high carbon/sulphur ratio might have produce abundant pyrite

clusters in a freshwater basin ([Hethke et al., 2013](#)). Also, the decomposition of organic matter by sulphate-reducing bacteria favoured increased acidity and would lead to the precipitation of early diagenetic pyrite ([Fürsich & Pan, 2016](#)). This sedimentological feature might be indicative of abundant decaying plant and animal remains consumed by bacteria at the lake bottom, but not for the redox state of the water column itself. However, a lacustrine palaeocoenosis, including ceratodontid lungfishes capable of aestivation in their burrows, horseshoe crabs, microdriles, and abundant microconchids, strongly supports a meromictic eutrophic lake.

Vacant ecological space is a key factor in allowing evolutionary innovation to develop ([Erwin, 2008](#)). Triassic austrolimulids capitalised on vacant marginal to freshwater environs left after the end-Permian extinction, thus exploiting an unprecedented array of niches and representing ‘disaster forms’ (sensu [Schubert & Bottjer, 1992](#)). Triassic forms exhibit more extreme morphologies than their Late Paleozoic counterparts (e.g., *Panduralimulus babcocki*, *Shpinevolimulus jakovlevi*, and *Tasmaniolimulus patersoni*) suggesting that the morphological stock required for Triassic diversification had arisen prior to the end-Permian ([Bicknell, 2019](#)). The high xiphosurid Triassic diversity and disparity, followed by a constrained morphology and generic level diversity from the Jurassic, records the extinction of austrolimulids ([Bicknell, Hecker & Heyng, 2021](#)) and the transition to a morphology that was conserved through into modern ecosystems ([Bicknell & Pates, 2020](#)). The hypertrophied genal spines observed in austrolimulids also illustrate evolutionary convergence with the Pennsylvanian-aged belinurids *Euproops* [Meek, 1867](#) and *Belinurus* [Pictet, 1846](#). The prevalence of this trait in two distinct xiphosurid families demonstrates how colonisation of marginal conditions placed similar evolutionary constraints on the xiphosurid body plan, resulting in comparable morphologies.

## ACKNOWLEDGEMENTS

We are deeply grateful to Anastasia Felker, Elena Lukashevich, Olesya Strelnikova, Maria Tarasenkova, Alexey Bashkuev and Dmitry Vasilenko who participated in fossil collecting, and especially to Eugeny Karasev who found the holotype, to Sergey Bagirov for the excellent photographs, to Roman Rakitov for his help in obtaining perfect SEM images, and to Andrey Sennikov (all PIN) and Valentin Tverdokhlebov (Saratov State University) for information on the fossil locality. We thank Nicolas E. Campione for discussions around the topic of disaster taxa and Katrina Kenny for her exceptional reconstruction of *Attenborolimulus superspinosus*. Finally, we thank Jason Dunlop, Joachim Haug, and Thomas Hegna for their comments that thoroughly improved the text.

## ADDITIONAL INFORMATION AND DECLARATIONS

### Funding

This research was supported by funding from a University of New England Postdoctoral Research Fellowship (to Russell D.C. Bicknell) and by the Russian Science Foundation grant 21-14-00284 (to Dmitry E. Shcherbakov). The funders had no role in study design, data collection and analysis, decision to publish, or preparation of the manuscript.

## Grant Disclosures

The following grant information was disclosed by the authors:  
University of New England Postdoctoral Research Fellowship.  
Russian Science Foundation: 21-14-00284.

## Competing Interests

The authors declare that they have no competing interests.

## Author Contributions

- Russell D.C. Bicknell conceived and designed the experiments, performed the experiments, analyzed the data, prepared figures and/or tables, authored or reviewed drafts of the paper, and approved the final draft.
- Dmitry E. Shcherbakov conceived and designed the experiments, performed the experiments, analyzed the data, prepared figures and/or tables, authored or reviewed drafts of the paper, and approved the final draft.

## Data Availability

The following information was supplied regarding data availability:

The raw morphometric data, the data needed to perform the analysis, and the PCA data are available in the [Supplementary Files](#).

Specimens are reposed in the Borissiak Paleontological Institute (PIN), Russian Academy of Sciences, Moscow, Russia:

PIN 5640/220 part and counterpart  
PIN 5640/200 part and counterpart  
PIN 5640/217

## New Species Registration

The following information was supplied regarding the registration of a newly described species:

Publication LSI: urn:lsid:zoobank.org:pub:5435A6BA-AE34-4698-8872-7A350DB799B1.

Genus name: urn:lsid:zoobank.org:act:11531F97-2ACA-411F-8002-E4E3426C22B6.

Species name: urn:lsid:zoobank.org:act:8FF20D49-096E-451E-9A06-284DC1665B1A.

## Supplemental Information

Supplemental information for this article can be found online at <http://dx.doi.org/10.7717/peerj.11709#supplemental-information>.

## REFERENCES

- Adams DC, Collyer ML, Kaliontzopoulou A. 2020. Geomorph: software for geometric morphometric analyses. R package version 3.2.1. Available at <https://cran.r-project.org/web/packages/geomorph/index.html>.
- Allen JG, Feldmann RM. 2005. *Panduralimulus babcocki* n. gen. and sp., a new Limulacean horseshoe crab from the Permian of Texas. *Journal of Paleontology* 79(3):594–600 DOI 10.1666/0022-3360(2005)079<0594:PBNGAS>2.0.CO;2.

- Benton MJ, Newell AJ.** 2014. Impacts of global warming on Permo-Triassic terrestrial ecosystems. *Gondwana Research* 25(4):1308–1337 DOI [10.1016/j.gr.2012.12.010](https://doi.org/10.1016/j.gr.2012.12.010).
- Benton MJ, Tverdokhlebov VP, Surkov MV.** 2004. Ecosystem remodelling among vertebrates at the Permian-Triassic boundary in Russia. *Nature* 432(7013):97–100 DOI [10.1038/nature02950](https://doi.org/10.1038/nature02950).
- Benton MJ, Zhang Q, Hu S, Chen Z-Q, Wen W, Liu J, Huang J, Zhou C, Xie T, Tong J.** 2013. Exceptional vertebrate biotas from the Triassic of China, and the expansion of marine ecosystems after the Permo-Triassic mass extinction. *Earth-Science Reviews* 125(5):199–243 DOI [10.1016/j.earscirev.2013.05.014](https://doi.org/10.1016/j.earscirev.2013.05.014).
- Bicknell RDC.** 2019. Xiphosurid from the Upper Permian of Tasmania confirms Palaeozoic origin of Austrolimulidae. *Palaeontologia Electronica* 22(3):1–13 DOI [10.26879/1005](https://doi.org/10.26879/1005).
- Bicknell RDC, Błażejowski B, Wings O, Hitij T, Botton ML.** 2021. Critical re-evaluation of Limulidae reveals limited Limulus diversity. *Papers in Palaeontology* 1–32 DOI [10.1002/spp2.1352](https://doi.org/10.1002/spp2.1352).
- Bicknell RDC, Brougham T, Charbonnier S, Sautereau F, Hitij T, Campione NE.** 2019a. On the appendicular anatomy of the xiphosurid *Tachypleus syriacus* and the evolution of fossil horseshoe crab appendages. *The Science of Nature* 106(7):38 DOI [10.1007/s00114-019-1629-6](https://doi.org/10.1007/s00114-019-1629-6).
- Bicknell RDC, Hecker A, Heyng AM.** 2021. New horseshoe crab fossil from Germany demonstrates post-Triassic extinction of Austrolimulidae. *Geological Magazine* 1–11 DOI [10.1017/S0016756820001478](https://doi.org/10.1017/S0016756820001478).
- Bicknell RDC, Naugolnykh SV, Brougham T.** 2020. A reappraisal of Paleozoic horseshoe crabs from Russia and Ukraine. *The Science of Nature* 107(5):46 DOI [10.1007/s00114-020-01701-1](https://doi.org/10.1007/s00114-020-01701-1).
- Bicknell RDC, Pates S.** 2019. Xiphosurid from the Tournaisian (Carboniferous) of Scotland confirms deep origin of Limuloidea. *Scientific Reports* 9(1):17102 DOI [10.1038/s41598-019-53442-5](https://doi.org/10.1038/s41598-019-53442-5).
- Bicknell RDC, Pates S.** 2020. Pictorial atlas of fossil and extant horseshoe crabs, with focus on Xiphosurida. *Frontiers in Earth Science* 8(98):60 DOI [10.3389/feart.2020.00098](https://doi.org/10.3389/feart.2020.00098).
- Bicknell RDC, Žalohar J, Miklavc P, Celarc B, Križnar M, Hitij T.** 2019b. A new limulid genus from the Strelivec Formation (Middle Triassic, Anisian) of northern Slovenia. *Geological Magazine* 156(12):2017–2030 DOI [10.1017/S0016756819000323](https://doi.org/10.1017/S0016756819000323).
- Błażejowski B, Niedźwiedzki G, Boukhalfa K, Soussi M.** 2017. *Limulitella tejraensis*, a new species of limulid (Chelicerata, Xiphosura) from the Middle Triassic of southern Tunisia (Saharan Platform). *Journal of Paleontology* 91(5):960–967 DOI [10.1017/jpa.2017.29](https://doi.org/10.1017/jpa.2017.29).
- Bleicher M-G.** 1897. Sur la découverte d'une nouvelle espèce de limule dans les marnes irisées de Lorraine. *Bulletin de la Societe des Sciences de Nancy* 2:116–126.
- Braun KFW.** 1860. Die Thiere in den Pflanzenschiefern der Gegend von Bayreuth. *Jahresbericht von der König Kreis-Landwirtschafts- und Gewerbschule zu Bayreuth für das Schuljahr 1859/60*:1–11.
- Chen Z-Q, Benton MJ.** 2012. The timing and pattern of biotic recovery following the end-Permian mass extinction. *Nature Geoscience* 5(6):375–383 DOI [10.1038/ngeo1475](https://doi.org/10.1038/ngeo1475).
- Chen Z-Q, Fraiser ML, Bolton C.** 2012. Early Triassic trace fossils from Gondwana Interior Sea: implication for ecosystem recovery following the end-Permian mass extinction in south high-latitude region. *Gondwana Research* 22(1):238–255 DOI [10.1016/j.gr.2011.08.015](https://doi.org/10.1016/j.gr.2011.08.015).
- Chu D, Tong J, Song H, Benton MJ, Song H, Yu J, Qiu X, Huang Y, Tian L.** 2015. Lilliput effect in freshwater ostracods during the Permian-Triassic extinction. *Palaeogeography, Palaeoclimatology, Palaeoecology* 435:38–52 DOI [10.1016/j.palaeo.2015.06.003](https://doi.org/10.1016/j.palaeo.2015.06.003).

- Crasquin-Soleau S, Galfetti T, Bucher H, Kershaw S, Feng Q.** 2007. Ostracod recovery in the aftermath of the Permian-Triassic crisis: Palaeozoic-Mesozoic turnover. *Hydrobiologia* **585**(1):13–27 DOI [10.1007/s10750-007-0625-6](https://doi.org/10.1007/s10750-007-0625-6).
- Crasquin S, Forel M-B.** 2014. Ostracods (Crustacea) through Permian-Triassic events. *Earth-Science Reviews* **137**(1):52–64 DOI [10.1016/j.earscirev.2013.01.006](https://doi.org/10.1016/j.earscirev.2013.01.006).
- Dineen AA, Fraiser ML, Sheehan PM.** 2014. Quantifying functional diversity in pre-and post-extinction paleocommunities: a test of ecological restructuring after the end-Permian mass extinction. *Earth-Science Reviews* **136**(3):339–349 DOI [10.1016/j.earscirev.2014.06.002](https://doi.org/10.1016/j.earscirev.2014.06.002).
- Dobruskina IA.** 1994. *Triassic Floras of Eurasia*. New York: Springer.
- Erwin DH.** 2008. Extinction as the loss of evolutionary history. *Proceedings of the National Academy of Sciences of the United States of America* **105**(Suppl. 1):11520–11527 DOI [10.1073/pnas.0801913105](https://doi.org/10.1073/pnas.0801913105).
- Erwin DH, Bowring SA, Yugan J.** 2002. End-Permian mass extinctions: a review. In: Koeberl C, MacLeod KC, eds. *Catastrophic Events and Mass Extinctions: Impacts and Beyond Special Paper* 356. Boulder: Geological Society of America, 363–384.
- Ewington DL, Clarke MJ, Banks MR.** 1989. A Late Permian fossil horseshoe crab (*Paleolimulus*: Xiphosura) from Poatina, Great Western Tiers. *Tasmania Papers and Proceedings of the Royal Society of Tasmania* **123**:127–131 DOI [10.26749/rstpp.123.127](https://doi.org/10.26749/rstpp.123.127).
- Forel M-B.** 2012. Ostracods (Crustacea) associated with microbialites across the Permian-Triassic boundary in Dajiang (Guizhou Province, south China). *European Journal of Taxonomy* **19**:1–34.
- Forel M-B, Crasquin S, Hips K, Kershaw S, Collin P-Y, Haas J.** 2013. Biodiversity evolution through the Permian—Triassic boundary event: Ostracods from the Bükk Mountains. *Hungary Acta Palaeontologica Polonica* **58**(1):195–219.
- Fu W, Jiang D-y, Montañez IP, Meyers SR, Motani R, Tintori A.** 2016. Eccentricity and obliquity paced carbon cycling in the Early Triassic and implications for post-extinction ecosystem recovery. *Scientific Reports* **6**(1):1–7 DOI [10.1038/s41598-016-0001-8](https://doi.org/10.1038/s41598-016-0001-8).
- Fürsich FT, Pan Y.** 2016. Diagenesis of bivalves from Jurassic and Lower Cretaceous lacustrine deposits of northeastern China. *Geological Magazine* **153**(1):17–37 DOI [10.1017/S0016756815000242](https://doi.org/10.1017/S0016756815000242).
- Gall J-C, Grauvogel-Stamm L.** 2005. The early Middle Triassic ‘Grès à Voltzia’ Formation of eastern France: a model of environmental refugium. *Comptes Rendus Palevol* **4**(6–7):637–652 DOI [10.1016/j.crpv.2005.04.007](https://doi.org/10.1016/j.crpv.2005.04.007).
- Glushenko NV, Ivanov VK.** 1961. *Paleolimulus* from the Lower Permian of the Donets Basin. *Paleontologiceskij Žurnal* **2**:128–130.
- Gomankov AV.** 2005. Floral changes across the Permian-Triassic boundary. *Stratigraphy and Geological Correlation* **13**(2):74–83.
- Hannibal JT, Shcherbakov DE.** 2019. New tomiulid millipedes from the Triassic of European Russia and a re-evaluation of the type material of *Tomiulus angulatus* from the Permian of Siberia. In: Dáni L, Korsós Z, Lazányi E, eds. *18th International Congress of Myriapodology: Hungarian Natural History Museum*. Budapest: Hungarian Biological Society, 25–31.
- Hauschke N, Wilde V.** 1987. *Paleolimulus fuchsbergensis* n. sp. (Xiphosura, Merostomata) aus der oberen Trias von Nordwestdeutschland, mit einer Übersicht zur Systematik und Verbreitung rezenter Limuliden. *Paläontologische Zeitschrift* **1**(2):87–108.
- Hethke M, Fürsich FT, Jiang B, Klaus R.** 2013. Oxygen deficiency in Lake Sihetun; formation of the Lower Cretaceous Liaoning Fossil Lagerstätte (China). *Journal of the Geological Society* **170**(5):817–831 DOI [10.1144/jgs2012-102](https://doi.org/10.1144/jgs2012-102).

- Hofmann R, Hautmann M, Wasmer M, Bucher H.** 2013. Palaeoecology of the Spathian Virgin Formation (Utah, USA) and its implications for the Early Triassic recovery. *Acta Palaeontologica Polonica* **58**(1):149–173.
- Hu S-X, Zhang Q-Y, Chen Z-Q, Zhou C-Y, Lü T, Xie T, Wen W, Huang J-Y, Benton MJ.** 2011. The Luoping biota: exceptional preservation, and new evidence on the Triassic recovery from end-Permian mass extinction. *Proceedings of the Royal Society B: Biological Sciences* **278**(1716):2274–2282.
- Hu S, Zhang Q, Feldmann RM, Benton MJ, Schweitzer CE, Huang J, Wen W, Zhou C, Xie T, Lü T, Hong S.** 2017. Exceptional appendage and soft-tissue preservation in a Middle Triassic horseshoe crab from SW China. *Scientific Reports* **7**(1):14112 DOI [10.1038/s41598-017-13319-x](https://doi.org/10.1038/s41598-017-13319-x).
- Jablonski D.** 2002. Survival without recovery after mass extinctions. *Proceedings of the National Academy of Sciences of the United States of America* **99**(12):8139–8144 DOI [10.1073/pnas.102163299](https://doi.org/10.1073/pnas.102163299).
- Kalandadze NN, Ochev VG, Tatarinov LP, Chudinov PK, Shishkin MA.** 1968. Katalog permeskikh i triasovykh tetrapod SSSR. *Doklady Akademii Nauk SSSR* **179**:72–91.
- Lamsdell JC.** 2020. The phylogeny and systematics of Xiphosura. *PeerJ* **8**:e10431 DOI [10.7717/peerj.10431](https://doi.org/10.7717/peerj.10431).
- Lange W.** 1923. Über neue Fossilfunde aus der Trias von Göttingen. *Zeitschrift der Deutschen Geologischen Gesellschaft* **74**:162–168.
- Lerner AJ, Lucas SG, Lockley M.** 2017. First fossil horseshoe crab (Xiphosurida) from the Triassic of North America. *Neues Jahrbuch für Geologie und Paläontologie-Abhandlungen* **286**(3):289–302 DOI [10.1127/njgpa/2017/0702](https://doi.org/10.1127/njgpa/2017/0702).
- Luo M, Chen ZQ.** 2014. New arthropod traces from the Lower Triassic Kockatea Shale Formation, northern Perth Basin, Western Australia: ichnology, taphonomy and palaeoecology. *Geological Journal* **49**(2):163–176 DOI [10.1002/gj.2506](https://doi.org/10.1002/gj.2506).
- Luo M, Shi GR, Buatois LA, Chen Z-Q.** 2020. Trace fossils as proxy for biotic recovery after the end-Permian mass extinction: a critical review. *Earth-Science Reviews* **203**(33):103059 DOI [10.1016/j.earscirev.2019.103059](https://doi.org/10.1016/j.earscirev.2019.103059).
- Luo M, Shi GR, Hu S, Benton MJ, Chen Z-Q, Huang J, Zhang Q, Zhou C, Wen W.** 2019. Early Middle Triassic trace fossils from the Luoping Biota, southwestern China: evidence of recovery from mass extinction. *Palaeogeography, Palaeoclimatology, Palaeoecology* **515**:6–22 DOI [10.1016/j.palaeo.2017.11.028](https://doi.org/10.1016/j.palaeo.2017.11.028).
- Lustri L, Laibl L, Bicknell RDC.** 2021. A revision of *Prolimulus woodwardi* Fritsch, 1899 with comparison to other paedomorphic belinurids. *PeerJ* **9**(4):e10980 DOI [10.7717/peerj.10980](https://doi.org/10.7717/peerj.10980).
- Meek FB.** 1867. Notes on a new genus of fossil Crustacea. *Geological Magazine, Decade 4*:320–321.
- Meischner K-D.** 1962. Neue Funde von *Psammolimulus gottingensis* (Merostomata, Xiphosura) aus dem Mittleren Buntsandstein von Göttingen. *Paläontologische Zeitschrift* **36**(1):185–193.
- Minikh MG, Minikh AV.** 1997. Ichthyofaunal correlation of the Triassic deposits from the northern Cis-Caspian and southern Cis-Urals regions. *Geodiversitas* **19**(2):279–292.
- Novikov IV.** 2018. Early Triassic amphibians of Eastern Europe: evolution of dominant groups and traits of changing communities (in Russian). *Transactions of Paleontological Institute, Russian Academy of Sciences* **296**:1–358.
- Ochev WG, Shishkin MA.** 1989. On the principles of global correlation at the continental Triassic on the tetrapods. *Acta Palaeontologica Polonica* **34**(2):149–173.

- Payne JL, Lehrmann DJ, Wei J, Orchard MJ, Schrag DP, Knoll AH.** 2004. Large perturbations of the carbon cycle during recovery from the end-Permian extinction. *Science* **305**(5683):506–509 DOI [10.1126/science.1097023](https://doi.org/10.1126/science.1097023).
- Pickett JW.** 1984. A new freshwater limuloid from the middle Triassic of New South Wales. *Palaeontology* **27**(3):609–621.
- Pictet F-J.** 1846. *Traité Élémentaire De Paléontologie Ou Histoire Naturelle Des Animaux Fossiles*. Paris: Baillière.
- Ponomarenko AG.** 1985. King crabs and eurypterids from the Permian and Mesozoic of the USSR. *Paleontological Journal* **19**:100–104.
- Ponomarenko AG.** 2016. Insects during the time around the Permian—Triassic crisis. *Paleontological Journal* **50**(2):174–186 DOI [10.1134/S0031030116020052](https://doi.org/10.1134/S0031030116020052).
- Riek EF.** 1955. A new xiphosuran from the Triassic sediments at Brookvale, New South Wales. *Records of the Australian Museum* **23**(5):281–282 DOI [10.3853/j.0067-1975.23.1955.637](https://doi.org/10.3853/j.0067-1975.23.1955.637).
- Riek EF.** 1968. Re-examination of two arthropod species from the Triassic of Brookvale, New South Wales. *Records of the Australian Museum* **27**(17):313–321 DOI [10.3853/j.0067-1975.27.1968.451](https://doi.org/10.3853/j.0067-1975.27.1968.451).
- Rodland DL, Bottjer DJ.** 2001. Biotic recovery from the end-Permian mass extinction: behavior of the inarticulate brachiopod *Lingula* as a disaster taxon. *Palaios* **16**(1):95–101 DOI [10.1669/0883-1351\(2001\)016<0095:BRFTEP>2.0.CO;2](https://doi.org/10.1669/0883-1351(2001)016<0095:BRFTEP>2.0.CO;2).
- Romero PA, Vía Boada L.** 1977. *Tarracolimulus rieki* nov. gen., nov. sp., nuevo Limulido del Triásico de Monreal-Alcover (Tarragona). *Cuadernos Geología Ibérica* **4**:239–246.
- Schimper W-P.** 1853. Palaeontologica alsatica: ou fragments paléontologiques des différents terrains stratifiés qui se rencontrent en Alsace. *Mémoires de la Société du Muséum d'Histoire Naturelle de Strasbourg* **4**:1–10.
- Schram FR.** 1979. Limulines of the Mississippian Bear Gulch Limestone of Central Montana, USA. *Transactions of the San Diego Society of Natural History* **19**(6):67–74.
- Schubert JK, Bottjer DJ.** 1992. Early Triassic stromatolites as post-mass extinction disaster forms. *Geology* **20**(10):883–886 DOI [10.1130/0091-7613\(1992\)020<0883:ETSAPM>2.3.CO;2](https://doi.org/10.1130/0091-7613(1992)020<0883:ETSAPM>2.3.CO;2).
- Shcherbakov DE.** 2008a. Insect recovery after the Permian/Triassic crisis. *Alavesia* **2**:125–131.
- Shcherbakov DE.** 2008b. On Permian and Triassic insect faunas in relation to biogeography and the Permian-Triassic crisis. *Paleontological Journal* **42**(1):15–31.
- Shcherbakov DE, Timm T, Tzetlin AB, Vinn O, Zhuravlev AY.** 2020. A probable oligochaete from an Early Triassic Lagerstätte of the southern Cis-Urals and its evolutionary implications. *Acta Palaeontologica Polonica* **65**(2):219–233 DOI [10.4202/app.00704.2019](https://doi.org/10.4202/app.00704.2019).
- Shcherbakov DE, Vinn O, Zhuravlev AY.** 2021. Disaster microconchids from the uppermost Permian and Lower Triassic lacustrine strata of the Cis-Urals and the Tunguska and Kuznetsk basins (Russia). *Geological Magazine* **1**–23 DOI [10.1017/S0016756820001375](https://doi.org/10.1017/S0016756820001375).
- Shi G, Woods AD, Yu M-Y, Li X-W, Wei H-Y, Qiao D.** 2019. Lower Triassic limulid trackways (*Kouphichnium*) from the southwestern margin of the Yangtze carbonate platform: paleoenvironmental and paleoecological implications. *Palaios* **34**(4):229–243 DOI [10.2110/palo.2018.081](https://doi.org/10.2110/palo.2018.081).
- Shishkin MA, Novikov IV.** 2017. Early stages of recovery of the East European tetrapod fauna after the end-Permian crisis. *Paleontological Journal* **51**(6):612–622 DOI [10.1134/S0031030117060089](https://doi.org/10.1134/S0031030117060089).
- Shishkin MA, Ochev VG, Tverdokhlebov VP, Vergay IF, Gomankov AV, Kalandadze NN, Leonova EM, Lopato AY, Makarova IS, Minikh MG, Molostovskiy EM, Novikov IV,**

**Sennikov AG.** 1995. *Biostratigrafiya kontinental'nogo triasa yuzhnogo Predural'ya* (*Biostratigraphy of the Continental Triassic in the Southern Cis-Urals*) (in Russian). Moscow: Nauka.

**Størmer L.** 1952. Phylogeny and taxonomy of fossil horseshoe crabs. *Journal of Paleontology* 26(4):630–640.

**Tintori A, Hitij T, Jiang D, Lombardo C, Sun Z.** 2014. Triassic actinopterygian fishes: the recovery after the end-Permian crisis. *Integrative Zoology* 9(4):394–411  
[DOI 10.1111/1749-4877.12077](https://doi.org/10.1111/1749-4877.12077).

**Tverdokhlebov VP.** 1967. Petropavlovka, Berezovy. In: Morozov NS, ed. *Putevoditel' ekskursii po verhnepermskim i triasovym kontinental'nym obrazovaniyam yugo-vostoka Russkoy platformy i Priural'ya* (Guidebook of the Excursion on Upper Permian and Triassic Continental Formations of the South-East of the Russian Platform and the Cis-Urals) (In Russian). Saratov: Saratovskiy Gosudarstvenny Universitet imeni N.G. Chernyshevskogo, Orenburgskoe Geologicheskoe Upravlenie.

**Tverdokhlebov VP.** 1987. Triasovye ozera Yuzhnogo Priural'ya (Triassic lakes of the southern Cis-Urals). In: Martinson GG, Neustrueva IY, eds. *Istoriya ozer pozdnego paleozooya i rannego mezozooya* (Late Palaeozoic and Early Mesozoic Lake History) (In Russian). Leningrad: Nauka, 235–242.

**Tverdokhlebov VP, Tverdokhlebova GI, Surkov MV, Benton MJ.** 2003. Tetrapod localities from the Triassic of the SE of European Russia. *Earth-Science Reviews* 60(1–2):1–66  
[DOI 10.1016/S0012-8252\(02\)00076-4](https://doi.org/10.1016/S0012-8252(02)00076-4).

**Twitchett RJ, Krystyn L, Baud A, Wheeley JR, Richoz S.** 2004. Rapid marine recovery after the end-Permian mass-extinction event in the absence of marine anoxia. *Geology* 32(9):805–808  
[DOI 10.1130/G20585.1](https://doi.org/10.1130/G20585.1).

**Vía Boada L.** 1987. Artropodos fosiles Triasicos de Alcover-Montral. II. *Limulidos*. *Cuadernos Geología Ibérica* 11:281–294.

**Vía L, De Villalta JF.** 1966. *Hetrolimulus gadeai*, nov. gen., nov. sp., représentant d'une nouvelle famille de Limulacés dans le Trias d'Espagne. *Comtes Rendues Sommaire Séances Société Géologique France* 8:57–59.

**von Fritsch KWG.** 1906. Beitrag zur Kenntnis der Tierwelt der deutschen Trias. *Abhandlungen der naturforschender Gesellschaft Halle* 24:220–285.

**Vorobyeva EI, Minikh MG.** 1968. Experimental application of biometry to the study of ceratodontid dental plates (in Russian). *Paleontological Journal* 2:76–87.

**Xing Z-F, Lin J, Fu Y-X, Zheng W, Liu Y-L, Qi Y-A.** 2021. Trace fossils from the Lower Triassic of North China—a potential signature of the gradual recovery of a terrestrial ecosystem. *Palaeoworld* 30(1):95–105 [DOI 10.1016/j.palwor.2020.06.002](https://doi.org/10.1016/j.palwor.2020.06.002).

**Zhang QY, Hu SX, Zhou CY, Lü T, Bai JK.** 2009. First occurrence of horseshoe crab (Arthropoda) fossils from China. *Progress in Natural Science* 19:1090–1093.

**Zheng D, Chang S-C, Wang H, Fang Y, Wang J, Feng C, Xie G, Jarzembski EA, Zhang H, Wang B.** 2018. Middle-Late Triassic insect radiation revealed by diverse fossils and isotopic ages from China. *Science Advances* 4(9):eaat1380 [DOI 10.1126/sciadv.aat1380](https://doi.org/10.1126/sciadv.aat1380).

**Żyła D, Wegierek P, Owocki K, Niedzwiedzki G.** 2013. Insects and crustaceans from the latest Early-early Middle Triassic of Poland. *Palaeogeography, Palaeoclimatology, Palaeoecology* 371:136–144 [DOI 10.1016/j.palaeo.2013.01.002](https://doi.org/10.1016/j.palaeo.2013.01.002).